

concentrations and temperature, and arrive at the unexpected conclusion that Eq. 2, and especially the heuristic crossover form Eq. 3, provide an excellent description of our data.

References and Notes

1. S. Sachdev, C. Buragohain, M. Vojta, *Science* **286**, 2479 (1999).
2. T. Matsuda, A. Fujioka, Y. Uchiyama, I. Tsukada, K. Uchinokura, *Phys. Rev. Lett.* **80**, 4566 (1998).
3. M. Azuma, Y. Fujishiro, M. Takano, M. Nohara, H. Takagi, *Phys. Rev. B* **55**, 8658 (1997).
4. M. Hücker et al., *Phys. Rev. B* **59**, R725 (1999).
5. B. Keimer et al., *Phys. Rev. B* **46**, 14034 (1992).
6. M. Corti et al., *Phys. Rev. B* **52**, 4226 (1995).
7. K. Uchinokura, T. Ino, I. Terasaki, I. Tsukada, *Physica B* **205**, 234 (1995).
8. D. Stauffer, A. Aharony, *Introduction to Percolation Theory, Revised 2nd Ed.* (Taylor and Francis, Bristol, PA, 1994).
9. M. E. J. Newman, R. M. Ziff, *Phys. Rev. Lett.* **85**, 4104 (2000).
10. R. J. Birgeneau, R. A. Cowley, G. Shirane, H. Yoshizawa, *J. Stat. Phys.* **34**, 817 (1984) and references therein.

11. C. Yasuda, A. Oguchi, *J. Phys. Soc. Jpn.* **68**, 2773 (1999).
12. Y.-C. Chen, A. H. Castro Neto, *Phys. Rev. B* **61**, R3772 (2000).
13. S. Miyashita, J. Behre, S. Yamamoto, in *Computational Approaches in Condensed Matter Physics*, S. Miyashita, M. Imada, H. Takayama, Eds. (Springer, Berlin, 1992), pp. 97–111.
14. K. Kato et al., *Phys. Rev. Lett.* **84**, 4204 (2000).
15. A. W. Sandvik, preprint available at <http://xxx.lanl.gov/abs/cond-mat/0110510>.
16. A. L. Chernyshev, Y. C. Chen, A. H. Castro Neto, preprint available at <http://xxx.lanl.gov/abs/cond-mat/0107488>.
17. R. J. Birgeneau et al., *Phys. Rev. B* **59**, 13788 (1999).
18. Y. J. Kim et al., *Phys. Rev. B* **64**, 4435 (2001).
19. M. Greven et al., *Z. Phys. B* **96**, 465 (1995).
20. B. B. Beard, R. J. Birgeneau, M. Greven, U.-J. Wiese, *Phys. Rev. Lett.* **80**, 1742 (1998).
21. S. Chakravarty, B. I. Halperin, D. R. Nelson, *Phys. Rev. B* **39**, 2344 (1989).
22. P. Hasenfratz, F. Niedermayer, *Phys. Lett. B* **268**, 231 (1991).
23. A. Aharony, R. J. Birgeneau, A. Coniglio, M. A. Kastner, H. E. Stanley, *Phys. Rev. Lett.* **60**, 1330 (1988).

24. K. Yamada et al., *Solid State Comm.* **64**, 753 (1987).
25. M. Greven, R. J. Birgeneau, *Phys. Rev. Lett.* **81**, 1945 (1998).
26. E. Manousakis, *Phys. Rev. B* **45**, 7570 (1992).
27. A. H. Castro Neto, D. Hone, *Phys. Rev. Lett.* **76** (1996).
28. A. B. Harris, S. Kirkpatrick, *Phys. Rev. B* **16**, 542 (1977).
29. R. Coldea et al., *Phys. Rev. Lett.* **86**, 5377 (2001).
30. H. E. Stanley, R. J. Birgeneau, P. J. Reynolds, J. F. Nicoll, *J. Phys. C* **9**, L553 (1976).
31. A. Coniglio, *Phys. Rev. Lett.* **46**, 250 (1981).
32. C. C. Wan, A. B. Harris, J. Adler, *J. Appl. Phys.* **69**, 5191 (1991).
33. O.P.V. and M.G. thank A. Aharony, A. H. Castro Neto, A. L. Chernyshev, A. W. Sandvik, and E. F. Shender for helpful discussions. The work at Stanford was supported by the U.S. Department of Energy under contract nos. DE-FG03-99ER45773 and DE-AC03-76SF00515, by NSF CAREER Award no. DMR9400372, and by the the A.P. Sloan Foundation.

15 October 2001; accepted 23 January 2002

Micro/Nano Encapsulation via Electrified Coaxial Liquid Jets

I. G. Loscertales,^{1*} A. Barrero,^{2*} I. Guerrero,² R. Cortijo,¹ M. Marquez,^{3,4} A. M. Gañán-Calvo²

We report a method to generate steady coaxial jets of immiscible liquids with diameters in the range of micrometer/nanometer size. This compound jet is generated by the action of electro-hydrodynamic (EHD) forces with a diameter that ranges from tens of nanometers to tens of micrometers. The eventual jet breakup results in an aerosol of monodisperse compound droplets with the outer liquid surrounding or encapsulating the inner one. Following this approach, we have produced monodisperse capsules with diameters varying between 10 and 0.15 micrometers, depending on the running parameters.

Production and control of droplets and particles of micrometer or even nanometer size with a narrow size distribution are of interest for many applications in science and technology. Usually, these particles are formed as either an aerosol or a hydrosol phase. Aerosols and hydrosols of compound particles, such that each particle is made of a small amount of a certain substance surrounded by another one, are of particular importance for encapsulation of food additives (1–3), targeted drug delivery (4–10), and special material processing (11, 12), among other technological fields. All of them resort to encapsulation

to provide such compound particles in the appropriate size range.

The interest in encapsulation may be motivated by a broad spectrum of reasons: to isolate an unstable component from an aggressive environment, to avoid decomposition of a labile compound under a certain atmosphere, to deliver a given substance to a particular receptor, and so forth. Although the substance to be encapsulated may be either solid or liquid, the encapsulating agent is usually a polymer carrying solution or a melted polymer. The key issue is the way to form the micrometer/nanometer-sized capsules from the bulk components, with controllable and adjustable coating thickness.

One of the most widely adopted methods to obtain micrometer/nanometer capsules is based on emulsion technology (13–15). Two immiscible fluids, one carrying the substance to be encapsulated and the other one carrying the polymer for the shell, are stirred to form an emulsion. This emulsion is stabilized by pouring it into a third solution (double emulsion process; DE), thereby extracting the

polymer solvent and solidifying the polymer as a capsule. Related methods also incorporate phase separation and similar physical or chemical phenomena (16, 17).

Other approaches for encapsulation resort to the formation and control of liquid jets with diameters in the micrometer/nanometer range. In the electrospray (ES) technique, a conducting liquid is slowly injected through an electrified capillary tube. When the electric potential between the liquid and its surroundings rises to a few kilovolts, the meniscus at the tube exit develops a conical shape, commonly referred to as the Taylor cone. A thin microthread of liquid is issued from the tip of the Taylor cone, which eventually fragments to form a spray of highly charged droplets (18). Its most well-known application has been in mass spectrometry, where it has been successfully exploited as a way to produce multiply charged gas phase ions of huge biomolecules present in the liquid phase (19). Another outstanding feature of the electrospray is its ability to generate monodisperse droplets whose size can be varied between hundred of micrometers and tens of nanometers, independent of the diameter of the capillary tube (20, 21).

In the simplest version of selective withdrawal (SW), the exit of a tube is located at a height S above the interface separating two immiscible liquids (or liquid gas). For low rates of fluid withdrawal Q , only the upper fluid is sucked through the tube. A sufficient increase in Q , or decrease in S , gives rise to a thin spout of the lower liquid surrounded by the outer fluid (22–24).

In the flow focusing (FF) technique (25, 26), a liquid is injected through a capillary tube whose exit is located close to a small hole drilled in a thin plate. A stream of another fluid (gas or liquid) surrounding the tube is forced through the hole. The mechan-

¹Escuela Técnica Superior de Ingenieros Industriales, Universidad de Málaga, Plaza El Ejido, S/N Málaga 29013, Spain. ²Escuela Superior de Ingenieros, Universidad de Sevilla, Camino de los Descubrimientos S/N, 41092 Sevilla, Spain. ³Kraft Foods R&D, The Nanotechnology Lab, 801 Waukegan Road, Glenview, IL 60025, USA. ⁴Los Alamos National Laboratory, Chemical Sciences and Technology Division, Los Alamos, NM 87545, USA.

*To whom correspondence should be addressed. E-mail: loscertales@uma.es; barrero@eurus2.us.es

ical stresses exerted by this stream deform the meniscus attached to the tube exit. Then, the meniscus develops a cusplike shape from whose vertex a thin jet is issued. As in the electrospray case, the jet diameter is also independent of the much larger diameter of the capillary tube.

In the DE methods, the capsules consist of a polymer matrix in which the encapsulated substance is somehow randomly distributed in tiny packets. The mean size of the capsules may vary between hundreds of nanometers and hundreds of micrometers, although the dispersion in sizes presents a relatively high standard deviation (usually larger than 100%).

Although each of these methods is able to produce encapsulated particles with a well-defined size range, good control over the thickness of the coating, or a specific size of coated particle, they are unable to accomplish all three of the desired parameters.

We report a technique that uses electrohydrodynamic (EHD) forces to generate coaxial jets of immiscible liquids with diameters in the nanometer range (27). The spray generated from the varicose breakup of the jet consists of monodisperse compound droplets, which can reach sizes well below the micrometer range. The basic experimental setup for the technique is sketched in Fig. 1. Two immiscible liquids, red and blue, are injected at appropriate flow rates through two concentrically located needles. The inner diameter of the inner needle ranges from the order of 1 mm to tens of micrometers, whereas its outer diameter sets limits to the cross section of the outer needle. The outer needle is connected to an electrical potential of several kilovolts relative to a ground electrode (the extractor). The inner needle is kept to an electrical potential that, depending on the conductivity of the outer liquid, can be varied from that of the outer needle to that of the extractor. For a

certain range of values of the electrical potential and flow rates (28), a structured Taylor cone is formed at the exit of the needles with an outer meniscus surrounding the inner one (see Fig. 2A). A liquid thread is issued from the vertex of each one of the two menisci, giving rise to a compound jet of two coflowing liquids (see Fig. 2B). At the minimum jet section, the two-layered jet shown in Fig. 2B has an outer diameter of 4 μm .

In the case of the experiment in Fig. 2, A and B, the outer liquid was DuPont photopolymer Somos 6120, and the inner one was colored ethylene glycol (EG). To develop this structure, we injected Somos, which flowed through the annular gap between the two needles. We then increased the electrical potential of the outer needle V_1 until the liquid meniscus jumped into a stable cone-jet mode. In this particular example, the electrical potential of the inner needle was maintained at $V_2 = V_1$. The viscosity of the outer liquid is sufficiently high to diffuse the electrical stresses acting on the surface into the bulk. Consequently, the liquid motion inside the Taylor cone is dominated by viscosity, so that the liquid velocity inside the cone is everywhere pointing toward the cone apex (29). The second liquid flowed through the inner needle to form a new meniscus inside the Somos one. The motion of Somos deformed the EG meniscus to a conical shape and sucked it from the meniscus's tip to form a thin microthread. This microthread of EG merged with that of Somos at the tip of the Taylor cone to finally form a two-concentric layered micro/nano jet.

To obtain a structured Taylor cone, the EHD forces must act on at least one liquid, although they may act on both. We shall call the driving liquid the one upon which the EHD forces act to form the Taylor cone. We introduced a configuration in which the driving liquid flows through the needle's annular gap (see

Fig. 1). However, there is an alternative configuration in which the driving liquid flows through T2, whereas the second one flows through the annular gap between T1 and T2. That is the case shown in Fig. 2, C and D, where a Taylor cone of water is formed inside a meniscus of a nonconducting liquid such as olive oil. The electrical stresses acting on the charged water-olive oil interface, which are efficiently transmitted by viscosity toward the olive oil bulk, set the olive oil into motion, toward the water cone vertex. These two coflowing streams eventually give rise to a coaxial jet of water coated by oil. As in regular electrosprays, the motion of the driving liquid in this second configuration does not need to be dominated by viscosity. Olive oil (or any other liquid insulator) cannot be electrosprayed on its own in the cone-jet mode, because the lack of surface charge density prevents the formation of a steady Taylor cone (30).

The stability of the structured Taylor cones and the electrified compound jets strongly depends on the physical properties of the working fluids as well as the liquid flow rates and applied voltages. This complex electro-fluid-mechanical scenario is rather poorly understood, so that the stability domains for most liquid couples remain to be investigated. In the absence of better knowledge, we should point out that stable structured Taylor cones have been obtained for liquids satisfying the condition $\sigma_i > \sigma_o$, where σ is the liquid-dielectric atmosphere surface tension and subscripts i and o refer to the inner and outer liquid, respectively.

Experiments show that the scaling laws (electrical current and droplet diameter as a function of flow rate) that govern regular electrosprays (20, 31, 32) also apply to these compound electrosprays. In this situation, the flow rate must be that of the driving liquid. For example, data in Fig. 3A, obtained by electrospraying water coated with oil, show a

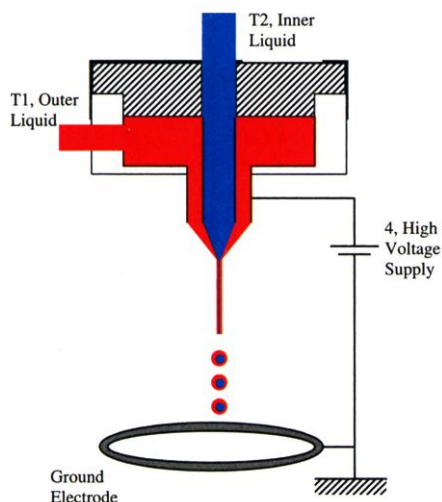


Fig. 1. Typical experimental setup for a structured Taylor cone.

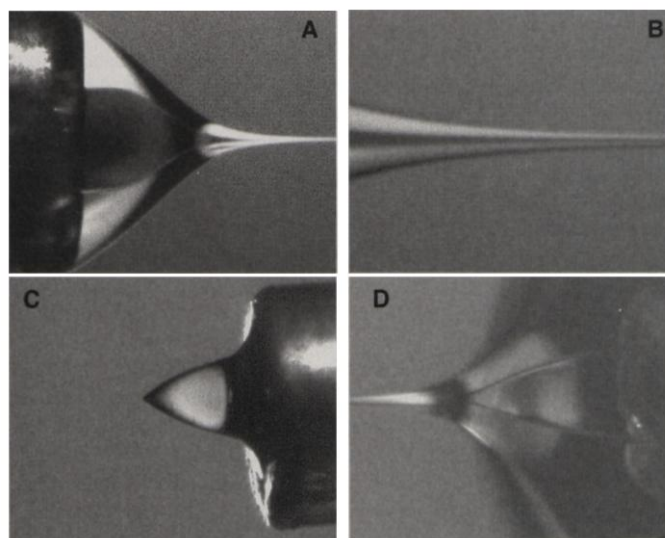


Fig. 2. (A) Structured Taylor cone and (B) downstream detail of the two coaxial jets emitted from the vertices of the two menisci. A Taylor cone of water coated by (C) a thin shell of olive oil and by (D) a thick shell of olive oil.

REPORTS

remarkable agreement with the well-known $I \sim Q^{1/2}$ law, where I is the current and the flow rate $Q = Q_{in}$ is, in this case, that of water (the driving liquid). Furthermore, as shown in Fig. 3B, the value of the current is not substantially affected by changes on the other liquid's flow rate, as far as both flow rates are comparable.

This behavior as regular electro spray is expected because, from the electrical point of view, the role played by the olive oil (insu-

lator) is exactly that played by air in regular electro sprays. The oil reduces the intensity of the electric field felt by the driving liquid (water) by a factor proportional to its dielectric constant, but, as with air, it makes no contribution to the net charge transport. Nonetheless, for much lower values of the oil flow rate, strong variations of I with Q_{out} have been found.

We applied this technique to microencapsulate aqueous solutions. An outer jet of So-

mos and a coflowing water inner jet were generated as described before. Compound droplets of water coated by Somos resulted from the jet breakup, so that a spray of compound droplets was formed and collected on a plate damped with water. In this case, the outer shell of the droplets was hardened with an ultraviolet light reactor. Before the hardening process, the charged aerosol was neutralized by corona discharge, so that losses were minimized. The liquid flow rates in this experiment were selected to obtain capsules in the micrometer range, because capsules in this range can be optically recorded to allow for visual observation (Fig. 4).

Encapsulation, tested within the nanometer range, has been carried out via aerosol techniques, because they allow for on-line characterization of the airborne particles. In particular, we resorted to mobility analysis with a differential mobility analyzer (DMA) described elsewhere (33). Electro spray droplets, when subject to sufficient liquid evaporation, lead to the formation of gas phase ions of substances previously dissolved in the liquid (34, 35), as in the case of aqueous solutions of salts.

In Fig. 5A, we show the differential mobility spectra recorded from an electro spray of an aqueous solution of NaCl. The liquid flow rate through the electro spray was 18 nl s^{-1} . The scale on the horizontal axis is proportional to I/Z , where Z is the electrical mobility in $\text{cm}^2 \text{ V}^{-1} \text{ s}^{-1}$. The leftmost peak is due to ions of sodium (Na^+) at different solvation states. The peak in the middle is mostly due to clusters of salt plus sodium ions at different states of charge and solvation (35). The third peak is due to the solid residues left after solvent evaporation from the droplets. Because the initially electro sprayed droplets evaporate and undergo Coulombic explosions, the sizes of the solid residues bear little relation to the initial droplet size, if any at all. In Fig. 5B, we show the differential mobility spectra gathered from the same aqueous solution, flowing at the same rate, but with 27% (in flow rate) of nonvolatile olive oil coflowing on the outside. The result is markedly different. The peaks associated with ions and ionic clusters have completely disappeared. There is only a single dominant peak, associated to the monodisperse electro spray compound droplets. Indeed, the size of such droplets, as inferred from the measured electric current and the liquid flow rate emitted from the electro spray, scales as those predicted by electro spray laws. Thus, the absence of ionic species and Coulomb explosions, together with the matching of predictions in size and charge, strongly supports the picture that the water droplets do not evaporate, so a thin shell of nonvolatile olive oil must surround them.

Figure 6 shows the diameter of the capsules generated from structured jets of olive oil (outer fluid) and water solutions (inner

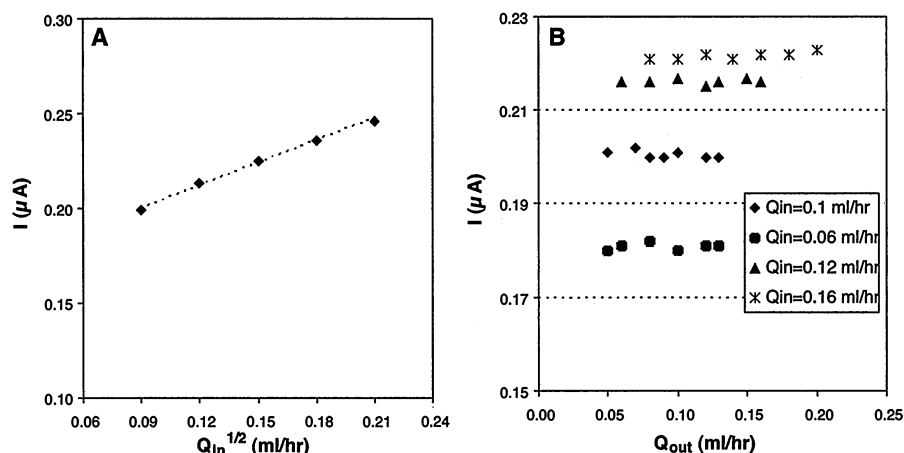


Fig. 3. (A) Current I as a function of the water flow rate Q_{in} for a given value of the oil flow rate Q_{out} . (B) Plot showing the independence of the current from Q_{out} .



Fig. 4. Collection of near monodisperse capsules. Magnified views of two capsules formed under different parametrical conditions are also given in the figure. In (A), the outer diameter is $10 \mu\text{m}$, whereas the diameter of the capsule shown in (B) is $8 \mu\text{m}$. The hardening process can also be thermally or chemically initiated under the use of appropriate reagents.

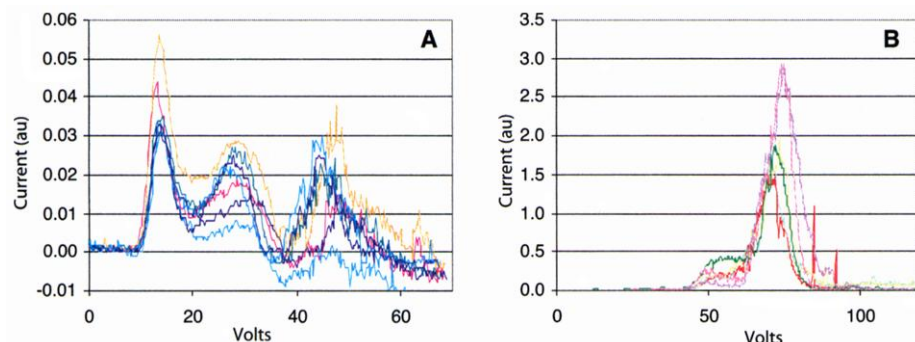
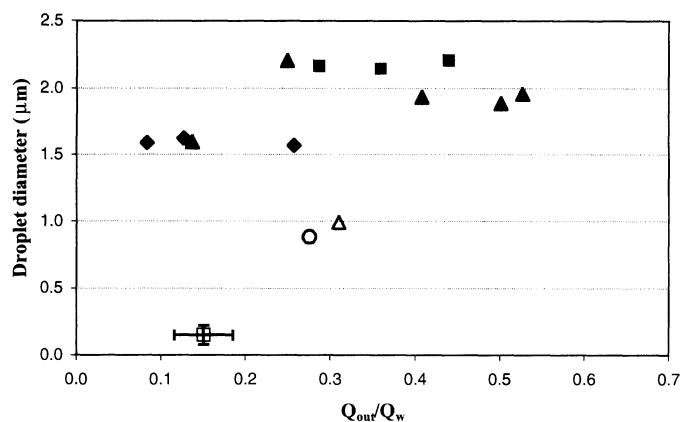


Fig. 5. Differential mobility spectra of (A) electro sprays of water solutions and (B) a compound electro spray of the same water solutions (inner) and olive oil (outer).

Fig. 6. Typical sizes of capsules of water surrounded by a thin shell of olive oil. ■, $Q_w = 39.8e-12 \text{ m}^3 \text{ s}^{-1}$; ▲, $Q_w = 26.0e-12 \text{ m}^3 \text{ s}^{-1}$; ◆, $Q_w = 18.4e-12 \text{ m}^3 \text{ s}^{-1}$; ○, $Q_w = 17.8e-12 \text{ m}^3 \text{ s}^{-1}$; △, $Q_w = 25.5e-12 \text{ m}^3 \text{ s}^{-1}$; and □, $Q_w = 1.5e-12 \text{ m}^3 \text{ s}^{-1}$.



fluid) with different electrical conductivities (0.14, 0.05, and 0.01 S m^{-1}). The horizontal axis represents the ratio Q_{out}/Q_w , where Q_w is the water flow rate and Q_{out} is the oil flow rate. The diameter is calculated from the measured current, flow rates, and electrical mobility. Filled symbols represent situations in which the flow rate of water is kept constant while the flow rate of olive oil is varied. Open symbols represent situations where both flow rates have been varied. The smallest capsule diameter attained during these exploratory experiments is about $0.150 \mu\text{m}$, corresponding to a sphere of water of about 100 nm in diameter covered by a layer of oil whose thickness is about 25 nm . The dispersion of sizes, for each experiment, remains below 7%, except in the case of the smallest capsules ($0.150 \mu\text{m}$), because of limitations to properly controlling the flow rate of oil in this extreme case.

We have presented a technique to generate coaxial electrified liquid jets in the micrometer and submicrometer ranges by EHD. This method allows for a precise tailoring of both the outer and the outer-to-inner radius ratio by controlling the flow rates of both liquids and the applied voltage. A direct application to the production of monodisperse capsules in the micrometer range has been included. Although in this particular example, the outer fluid consists of a photopolymer, which is solidified under ultraviolet light, the use of different polymerization schemes is also applicable with this technique. Also, monodisperse compound droplets of water coated by olive oil, with sizes well in the submicrometer range, have been obtained. Both the amount of water and thickness of the coating oil layer can be well controlled.

References and Notes

- H. Yosii et al., *Inn. Food Sci. Em. Technol.* **2**, 55 (2001).
- N. Hardas, S. Danviriyakul, J. L. Foley, W. W. Nawar, P. Chinachoti, *Lebensm.-Wiss. U.-Technol.* **33**, 506 (2000).
- S. J. Lee, M. Rosemberg, *Lebensm.-Wiss. U.-Technol.* **33**, 80 (2000).
- G. H. Wolters, W. M. Fritschy, D. Gerrits, R. Van Schilffgaarde, *J. Appl. Biomatter* **3**, 281 (1992).
- E. Mathiowitz, *Encyclopedia of Controlled Drug Delivery* (Wiley, New York, 1999).

- E. Mathiowitz et al., *Nature* **386**, 410 (1997).
- T. Jung et al., *Eur. J. Pharm. Biopharm.* **50**, 147 (2000).
- R. T. Bartus, M. A. Tracy, D. F. Emerich, S. E. Zale, *Science* **281**, 1161 (1998).
- R. Langer, *Nature* **392**, 5 (1998).
- T. Ciach, J. Wang, J. Marijnissen, *J. Aerosol Sci.* **32**, S1001 (2001).
- Y. H. Lee, C. A. Kim, W. H. Jang, H. J. Choi, M. S. Jhon, *Polymer* **42**, 8277 (2001).
- G. Burlak, S. Koshevaya, J. Sánchez-Mondragón, V. Grimalsky, *Opt. Commun.* **187**, 91 (2001).
- R. A. Jain, *Biomaterials* **21**, 2475 (2000).
- R. Gref et al., *Science* **263**, 1600 (1994).
- M. Aboubakar, F. Puisieux, P. Couvreur, C. Vauthier, *Int. J. Pharm.* **183**, 63 (1999).
- G. E. Hildebrand, J. W. Tack, *Int. J. Pharm.* **196**, 173 (2000).
- H. Reithmeier, J. Herrmann, A. Göpferich, *Int. J. Pharm.* **218**, 133 (2001).
- M. Cloupeau, B. Prunet-Foch, *J. Aerosol Sci.* **25**, 1021 (1994).
- J. B. Fenn, M. Mann, C. K. Meng, S. F. Wong, *Science* **246**, 64 (1989).
- A. M. Gañán-Calvo, J. Dávila, A. Barrero, *J. Aerosol Sci.* **28**, 249 (1997).
- I. G. Loscertales, J. Fernández de la Mora, in *Synthesis and Measurement of Ultrafine Particles*, J. Marijnissen, S. Pratsinis, Eds. (Delft Univ. Press, Delft, Netherlands, 1993), pp. 115–118.
- J. R. Lister, *J. Fluid Mech.* **198**, 231 (1989).

- S. Blake, G. N. Ivey, *J. Volcanol. Geotherm. Res.* **27**, 153 (1986).
- I. Cohen, H. Li, J. L. Houglund, M. Mrksich, S. R. Nagel, *Science* **292**, 265 (2001).
- A. M. Gañán-Calvo, *Phys. Rev. Lett.* **80**, 285 (1997).
- _____, A. Barrero, *J. Aerosol Sci.* **30**, 117 (1999).
- I. G. Loscertales, R. Cortijo, A. Barrero, A. M. Gañán-Calvo, Spanish Patent Application P2001-00231 (2001).
- The range of values of the applied electrical potential and injected flow rates required to obtain a structured Taylor cone depends on the physical properties of the liquids (mainly electrical conductivities, viscosities, and surface tensions; $6.2 \times 10^{-5} \text{ S m}^{-1}$ and $0.6 \text{ kg m}^{-1} \text{ s}^{-1}$ are the electrical conductivity and viscosity of Somos, and 43 mN m^{-1} is the Somos-air interfacial tension) and the geometry of the system (mainly the needle-to-collector distance). In our experiments, the diameters of the needles were 1 mm outer diameter (OD) and 0.7 mm inner diameter (ID) (outer needle) and 0.4 mm OD and 0.25 mm ID (inner needle). Silica tubing (0.35 mm OD, 0.075 mm ID) was also used as the inner needle in the experiments with water-oil. The needle-to-collector distance ranged between about 0.8 and 1.4 mm . Typical values of the voltages used in the experiments shown in Figs. 2 to 6 range between 3 and 5 kV . Typical values of the liquid flow rates are given in Figs. 3 and 6.
- The use of liquids with much less viscosity may lead to intense flow recirculations inside the Taylor cone (36).
- The only way liquid insulators can be electrospayed in the cone-jet mode is by artificially increasing their electrical conductivity via additives.
- J. Fernández de la Mora, I. G. Loscertales, *J. Fluid Mech.* **260**, 155 (1994).
- J. Rosell-Llompart, J. Fernández de la Mora, *J. Aerosol Sci.* **25**, 1093 (1994).
- J. Rosell-Llompart, I. G. Loscertales, D. Bingham, J. Fernández de la Mora, *J. Aerosol Sci.* **27**, 695 (1996).
- I. G. Loscertales, J. Fernández de la Mora, *J. Chem. Phys.* **103**, 5041 (1995).
- M. Gamero-Castaño, J. Fernández de la Mora, *Anal. Chim. Acta* **406**, 67 (2000).
- A. Barrero, A. M. Gañán-Calvo, J. Dávila, A. Palacio, E. Gómez-González, *Phys. Rev. E* **58**, 7309 (1998).
- Two of the authors (I.G.L.) and (A.B.) thank J. Fernández de la Mora, J. M. López-Herrera, A. Garrido, and M. González for their valuable assistance. One of the authors (M.M.) dedicates this work to G. Chuchani on his 77th anniversary.

31 October 2001; accepted 24 January 2002

A Thermally Re-mendable Cross-Linked Polymeric Material

Xiangxu Chen,¹ Matheus A. Dam,¹ Kanji Ono,² Ajit Mal,³ Hongbin Shen,⁴ Steven R. Nutt,⁴ Kevin Sheran,¹ Fred Wudl^{1*}

We have developed a transparent organic polymeric material that can repeatedly mend or "re-mend" itself under mild conditions. The material is a tough solid at room temperature and below with mechanical properties equaling those of commercial epoxy resins. At temperatures above 120°C , approximately 30% (as determined by solid-state nuclear magnetic resonance spectroscopy) of "intermonomer" linkages disconnect but then reconnect upon cooling. This process is fully reversible and can be used to restore a fractured part of the polymer multiple times, and it does not require additional ingredients such as a catalyst, additional monomer, or special surface treatment of the fractured interface.

In past decades, highly cross-linked polymers have been studied widely as matrices for composites, foamed structures, structural adhesives, insulators for electronic packaging, etc. (1, 2). The densely cross-linked structures are the basis of superior mechanical

properties such as high modulus, high fracture strength, and solvent resistance. However, these materials are irreversibly damaged by high stresses (3, 4) due to the formation and propagation of cracks. The latter lead to dangerous loss in the load-carrying capacity of poly-